Bioimaging

Deutsche Ausgabe: DOI: 10.1002/ange.201601122
Internationale Ausgabe: DOI: 10.1002/anie.201601122

Molecularly Imprinted Polymer Coated Quantum Dots for Multiplexed Cell Targeting and Imaging

Maria Panagiotopoulou, Yolanda Salinas, Selim Beyazit, Stephanie Kunath, Luminita Duma, Elise Prost, Andrew G. Mayes, Marina Resmini, Bernadette Tse Sum Bui, and Karsten Haupt**

Abstract: *Advanced tools for cell imaging are of great interest for the detection, localization, and quantification of molecular biomarkers of cancer or infection. We describe a novel photopolymerization method to coat quantum dots (QDs) with polymer shells, in particular, molecularly imprinted polymers (MIPs), by using the visible light emitted from QDs excited by UV light. Fluorescent core–shell particles specifically recognizing glucuronic acid (GlcA) or N-acetylneuraminic acid (NANA) were prepared. Simultaneous multiplexed labeling of human keratinocytes with green QDs conjugated with MIP-GlcA and red QDs conjugated with MIP-NANA was demonstrated by fluorescence imaging. The specificity of binding was verified with a non-imprinted control polymer and by enzymatic cleavage of the terminal GlcA and NANA moieties. The coating strategy is potentially a generic method for the functionalization of QDs to address a much wider range of biocompatibility and biorecognition issues.*

Fluorescent semiconductor nanocrystals, so-called quantum dots (QDs), have unique optical and electronic properties: size-tunable light emission, high signal brightness with reduced photobleaching, long-term photostability, and possible multiplexing due to narrow, symmetric, and well-resolved emission spectra. They have broad absorption spectra which enable simultaneous excitation of multiple QDs by a common excitation wavelength. QDs have been used as luminescent probes in bioassays, biosensors, and medical diagnostics,[1–4] such as cell imaging for cancer detection.[5–7] QD nanocrystals are generally synthesized in apolar solvents and are hydrophobic. Substantial progress in surface chemistry for rendering them soluble in aqueous media has been the key to their biocompatibility and functionalization for the coupling of specific affinity ligands (antibodies, nucleic acids, peptides). Different QD-solubilization strategies have been devised, including ligand exchange with small monodentate or polydentate thiol-containing molecules and encapsulation by a layer of amphiphilic polymers, polysaccharides, or proteins, silica shells, and phospholipid micelles.[1,2,4,8]

Herein, we present a novel versatile solubilization and functionalization strategy, which consists of creating a stable and robust hydrophilic cross-linked polymer coating directly on QDs by photopolymerization using the particles as individual internal light sources. Green- and red-emitting InP/ZnS QDs, hereafter referred to as green-QDs and red-QDs, which are less toxic than cadmium-based QDs,[7,9] were employed. Emitted fluorescent light from green (550 nm) or red QDs (660 nm), when excited with a UV lamp (365 nm), locally photopolymerizes a thin polymer shell on the surface of the QDs, thus yielding core–shell nanoparticles (Figure 1 A).

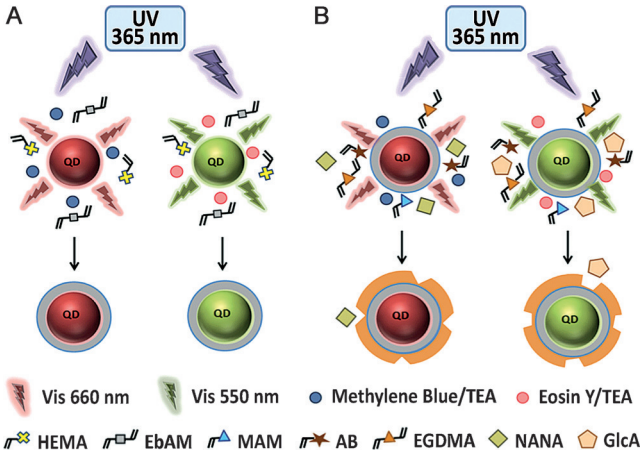

Figure 1. A) Red or green light emitted from InP/ZnS quantum dots excited by UV irradiation is used to synthesize a polymeric shell in situ around the particles by photopolymerization. Methylene blue/triethylamine (TEA) are used as the initiator system for red-QDs and eosin Y/TEA for green-QDs. B) A second shell of MIP is synthesized by reinitiation in the presence of functional and cross-linking monomers and a molecular template (GlcA or NANA).

Since emission from QDs is weak as compared to direct light, polymerization is confined to the QD surface; however, appropriate initiator systems must be used.[10] The emission

[*] M. Panagiotopoulou, Dr. S. Beyazit, Dr. S. Kunath, Dr. L. Duma, E. Prost, Dr. B. Tse Sum Bui, Prof. K. Haupt
Sorbonne Universités, Université de Technologie de Compiègne
CNRS Enzyme and Cell Engineering Laboratory
Rue Roger Couttolenc, CS 60319, 60203 Compiègne Cedex (France)
E-mail: jeanne.tse-sum-bui@utc.fr
karsten.haupt@utc.fr
Homepage: http://www.utc.fr/mip
Dr. Y. Salinas, Prof. M. Resmini
School of Biological and Chemical Sciences
Queen Mary University of London
London E1 4NS (UK)
Dr. A. G. Mayes
School of Chemistry, University of East Anglia
Norwich Research Park, Norwich NR4 7TJ (UK)

Supporting information for this article, including experimental details (reagents and materials, synthesis and characterization of MIP-QDs, equilibrium and competitive binding assays, TEM and DLS analysis, ^{1}H NMR studies of the AB–template complex, and cell and tissue staining and imaging), can be found under: http://dx.doi.org/10.1002/anie.201601122.

wavelength of the QD must overlap with the absorption wavelength of the initiator (see Figures S1 and S2 A in the Supporting Information), and the latter must not be activated by the UV light. Preliminary experiments confirmed that these requirements are met in the systems described (Figure 1; see the Supporting Information for details). At the same time, we verified that there was no self-initiated polymerization, a phenomenon frequently observed in the presence of numerous monomers and under lower-wavelength UV light.[11]

A MIP shell specific for glucuronic acid (GlcA; green-QDs) or *N*-acetylneuraminic acid (NANA; red-QDs) was grafted on top of the hydrophilic first shell (Figure 1 B) to target glycosylation sites on cells, since altered glycosylation levels or distributions are indicators of infection or malignancy. Recent advances in glycobiology and cancer research have defined the key processes underlying aberrant glycosylation with sialic acids or hyaluronan in cancer and its consequences.[12–15] Consequences include effects on tumor growth, escape from apoptosis, metastasis formation, and resistance to therapy. Polysaccharides involved in the glycosylation procedure have a highly conserved simple composition and are ubiquitously expressed in all animals that have a developed immune response. The natural production of antibodies that specifically recognize these "weak antigens" is difficult;[16] hence, traditional immunohistochemical methods for detecting glycosylations on cells are rare. An alternative would be "plastic antibodies" or MIPs.[17,18] MIPs are tailor-made synthetic antibody mimics that can recognize and bind target molecules specifically. They are synthesized by copolymerizing functional and cross-linking monomers in the presence of a molecular template, thus resulting in the formation of binding sites with affinities and specificities comparable to those of natural antibodies. Their molecular-recognition properties, combined with a high chemical and physical stability, make them interesting substitutes for antibodies in immunoassays,[19] biosensors,[20] bioseparation,[18,21] controlled drug release,[22] and bioimaging.[23–25]

In this study, MIP-coated QDs were applied for the first time for the simultaneous multiplexed pseudoimmunolabeling and imaging of human keratinocytes. Core–shell MIP nanoparticles for GlcA and NANA, (125 ± 17) nm in size, were obtained, thus enabling the specific targeting of both intracellular and pericellular terminal glycosylations. We previously reported 400 nm rhodamine-labeled MIP particles specific for GlcA that could only target the extracellular hyaluronan of the cell glycocalix.[23] We have now synthesized a dedicated stoichiometric functional monomer,[26] (4-acrylamidophenyl)(amino)methaniminium acetate, a polymerizable benzamidine referred to as AB in the text (see the Supporting Information for the synthesis of AB; see also Figure S3), which can form strong electrostatic interactions with the −COOH moiety of GlcA and NANA. Commonly, boronate-based monomers are employed[25,27] for targeting NANA and other monosaccharides, but the use of only noncovalent interactions is preferred for sugar imprinting in terms of binding and exchange kinetics.[28]

Green-QDs were prepared according to a previous report (see the Supporting Information).[29] A water-compatible shell was synthesized by using the hydrophilic monomers 2-hydroxyethyl methacrylate (HEMA) and *N*,*N*′-ethylene-bis(acrylamide) (EbAM), the initiator couple eosin Y/triethylamine (TEA), and green-QDs in toluene/dimethyl sulfoxide (DMSO; 1:1). This shell stabilizes the QDs for their further conjugation in polar solvents. Its presence (HEMA-QDs) was confirmed by transmission electron microscopy (TEM) and dynamic light scattering (DLS) (Figure 2 A,B). Further evidence was provided by another

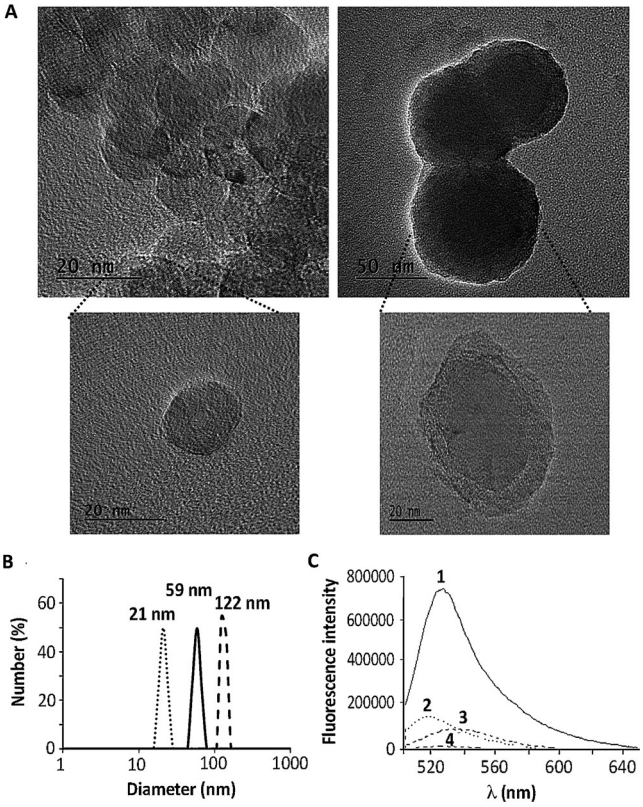

Figure 2. Evidence for the formation of a polymer shell around green-QDs. A) TEM images of bare QDs (left) and HEMA-QDs (right). B) Size distribution as measured by DLS of bare QDs (dotted line), HEMA-QDs (solid line), and MIPGlcA-QDs (dashed line). C) Emission spectra ($\lambda_{ex} = 495$ nm) of propargyl-functionalized QDs before (4) and after fluorescein labeling (1). The presence of fluorescein ($\lambda_{em} = 525$ nm) was clearly visible after labeling, whereas in control experiments with bare QDs, no fluorescein was seen before (2) or after labeling (3).

experiment, in which propargyl acrylamide was added to the polymerization mixture described above. The resulting propargyl-functionalized shell was then labeled with azidofluorescein (see the Supporting Information for synthetic details) by click chemistry. Fluorescein ($\lambda_{ex} = 495$ nm) was incorporated, as shown by the emission spectrum of the core–shell particles (Figure 2 C).

A MIP was photopolymerized on top of the first shell, again by using green light emitted by the QDs. The HEMA-QD particles were resuspended in DMSO, and the second shell (MIPGlcA-QDs) was obtained by irradiation with UV light using an MIP-precursor mixture containing GlcA, AB,

methacrylamide (MAM), ethylene glycol dimethacrylate (EGDMA), and eosin/TEA. MAM was added to provide hydrogen-bonding interactions with GlcA and to render the MIP more hydrophilic to prevent aggregation in the aqueous cell-imaging medium. A control non-imprinted polymer (NIP) was prepared in the same way but without the addition of GlcA. The stoichiometry and binding constant of the AB–GlcA complex were deduced from NMR titration studies in [D_6]-DMSO, which yielded a 1:1 ratio and a high association constant (K_a) of $7.1 \times 10^3\,\text{M}^{-1}$ (see Figure S4).

The recognition properties of MIPGlcA-QDs were evaluated by equilibrium radioligand-binding assays with [^{14}C]glucuronic acid in water. Figure 3A shows that MIPGlcA-QDs bound much more GlcA than NIPGlcA-QDs, thus indicating the creation of imprinted sites. MIP

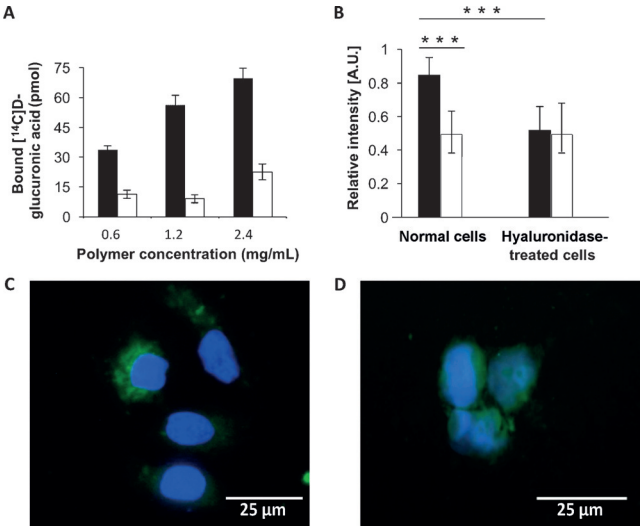

Figure 3. A) Equilibrium binding assay of MIPGlcA-QDs (black) and NIPGlcA-QDs (white) with [^{14}C]glucuronic acid in water. B) Relative fluorescence intensity of keratinocytes after imaging with MIP-QDs (black) and NIP-QDs (white), with and without hyaluronidase treatment ($n = 4$ independent replicates with quadruplicates for each experiment). Mean values of MIP and NIP for normal cells, and of MIP for normal cells and MIP for hyaluronidase-treated cells, are significantly different at 99.9% confidence ($p \leq 0.001$***). C, D) Staining of keratinocytes (C) and KU812 cells (D) with MIP-QDs (green); nuclear staining with 4′,6-diamidino-2-phenylindole (DAPI; blue).

selectivity was confirmed by competitive binding assays comparing the binding of GlcA with that of other monosaccharides, such as *N*-acetylgalactosamine, *N*-acetylglucosamine, galactose, glucose, and NANA, present in the terminal parts of glycolipids or glycoproteins that could potentially interfere during cell imaging. Since a large amount of particles are needed for competition studies, MIPGlcA and MIP-NANA polymers obtained by precipitation polymerization were employed instead of MIP-coated QDs. Less than 1% cross-reactivity was observed (see Figure S6 and Table S1).

For quantitative cell imaging, a standard immunostaining protocol was adopted for visualizing the MIP-QDs on human keratinocytes (HaCaT cells). To avoid possible interference from the fluorescence of entrapped residual eosin Y, the dye was photobleached prior to imaging experiments (see the Supporting Information for details). After cell fixation, MIPGlcA-QDs were added and left to incubate for 90 min before imaging (Figure 3C). Fluorescent particles on the cells were quantified after background subtraction by epifluorescence microscopy (see the Supporting Information for sample preparation, cell fixation, and fluorescent-image analysis). MIPGlcA-QDs showed 42% more binding to the cells than NIPGlcA-QDs (Figure 3B). MIPGlcA-QDs were also applied to another cell type, leukemia KU812, thus showing the versatility of the staining method (Figure 3D).

To confirm the selectivity of MIP-QD staining, we treated cells with hyaluronidase to remove terminal glucuronic acid moieties from the glycosylation sites (see Figure S8). Quantitative analysis of images revealed a 40% reduction in the fluorescence signal of hyaluronidase-treated versus untreated cells, whereas no change was observed for NIP-QD stained cells (Figure 3B). These results were validated by comparison with a previously reported method with a biotinylated hyaluronic acid binding protein (HABP).[30] The protein was revealed with fluorescein isothiocyanate labeled streptavidin. Quantitative analysis of the images revealed a 52% reduction in the fluorescence signal of hyaluronidase-treated versus untreated cells (see Figure S10), which is comparable to the reduction in recognition observed with MIPs.

To prove the versatility of our method for functionalizing QDs, commercially available red-QDs emitting at 660 nm were tested. Methylene blue/TEA was used for initiation to ensure spectral overlap between QD emission and initiator absorption. A HEMA/EbAM shell was grafted around the QDs, followed by a MIPNANA shell, by the same procedure as described for green-QDs. The polymers were then photobleached to eliminate any methylene blue fluorescence. The increase in size of the QDs after coating was verified by DLS measurements (see Figure S2B). The stoichiometry and binding constant of the AB–NANA complex were obtained by NMR titration studies in [D_6]-DMSO, which yielded a 1:1 ratio and a high K_a value of $41 \times 10^3\,\text{M}^{-1}$ (see Figure S5).

The specificity of MIPNANA-QDs was evaluated by equilibrium binding assays with [^{3}H]sialic acid in water. MIPNANA bound more sialic acid than NIPNANA (Figure 4A), thus indicating the creation of imprinted sites. Competitive equilibrium binding assays showed that there was $< 10\%$ cross-reactivity with GlcA and negligible cross-reactivity with other terminal sugars: *N*-acetylglucosamine, *N*-acetylgalactosamine, galactose, and glucose (see Figure S7 and Table S1). In quantitative cell imaging, MIPNANA-QDs showed 48% more binding than NIPNANA-QDs. MIP staining specificity was confirmed by enzymatic treatment of the cells with neuraminidase (see Figure S9), which yielded a fluorescence profile similar to that of NIP-QD stained cells (Figure 4B).

Our next step was to investigate whether multiplexed imaging of GlcA and NANA on fixed keratinocytes was possible. The spatial distribution of MIP-QDs targeting GlcA or NANA on keratinocytes was determined with epifluorescence microscopy (Figures 3C and 4C). As expected, the particles were found almost exclusively in regions where cells were present. Confocal microscopy was then used to study the

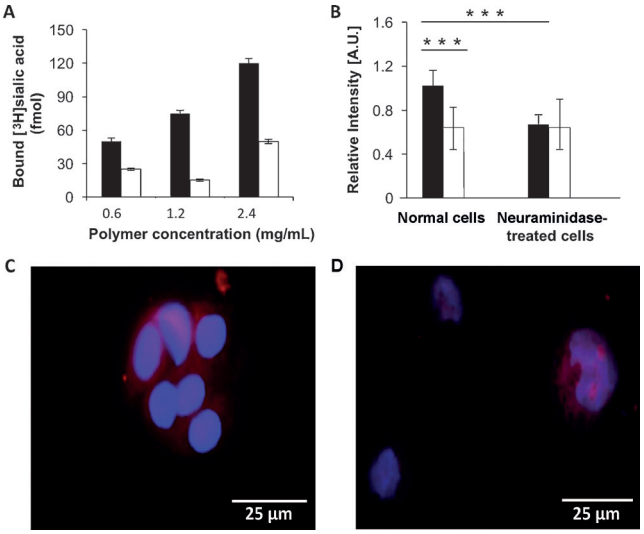

Figure 4. A) Equilibrium binding assay of MIPNANA-QDs (black) and NIPNANA-QDs (white) with [^{3}H]sialic acid in water. B) Relative fluorescence intensity of keratinocytes after imaging with MIP-QDs (black) and NIP-QDs (white), with and without neuraminidase treatment ($n = 4$ independent replicates with quadruplicates in each experiment). Mean values of MIP and NIP for normal cells, and of MIP for normal cells and MIP for hyaluronidase-treated cells, are significantly different at 99.9% confidence ($p \leq 0.001$***). C, D) Staining of keratinocytes (C) and KU812 (D) with MIP-QDs (red); nuclear staining with DAPI (blue).

distribution of MIP-QDs along the z axis. The MIPGlcA-QDs (green) were localized extracellularly, pericellularly, and intracellularly, even within the nucleus in some cases (see Figure S11 A). Nuclear staining, due to the distribution of hyaluronan in nuclear clefts, has been reported previously.[31] MIPNANA-QDs (red) were localized mainly extra- and pericellularly (see Figure S11 B), in accord with the localization of terminal sialic acids in human cells.[24,32] The use of organic dyes to stain the nucleus shows that MIP-QD staining can be readily coupled with other staining methods without interference or loss of specificity (Figure 5). This study demonstrates for the first time the potential of molecularly imprinted polymers when conjugated to quantum dots of different emission colors as a versatile multiplexed imaging tool.

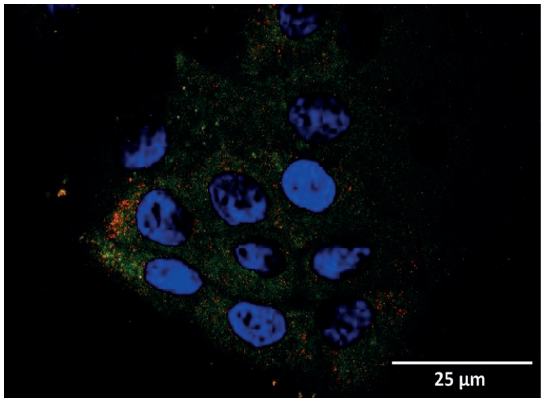

Figure 5. Confocal microscope image showing simultaneous multiplexed staining of GlcA and NANA on human keratinocytes by MIPGlcA-QDs (green) and MIPNANA-QDs (red). Nuclear staining with DAPI (blue).

In conclusion, we have developed a convenient and generic strategy to coat QDs with thin polymer shells to impart functionalization and biocompatibility by photopolymerization using the visible fluorescent light emitted from QDs upon excitation by UV light. MIP-coated QDs imprinted with glucuronic and *N*-acetylneuraminic acid were used for the recognition of hyaluronic acid and sialylated glycoproteins and glycolipids on keratinocytes as an illustrative example of the multiplexed detection of glycosylations in cells. The application of MIP-coated QDs as artificial receptors and imaging agents for glycosylation sites paves the way for new applications in diagnostics, theranostics, and therapeutics.

Acknowledgments

This research was supported by the European Regional Development Fund, the Region of Picardy (CPER 2007–2013), and the European Commission (FP7 Marie Curie Actions, projects NANODRUG, MCITN-2011-289554, and SAMOSS, PITN-2013–607590). We thank F. Nadaud and C. Boulnois for TEM measurements.

Keywords: bioimaging · molecularly imprinted polymers · nanocomposites · quantum dots · synthetic receptors

How to cite: *Angew. Chem. Int. Ed.* **2016**, *55*, 8244–8248
Angew. Chem. **2016**, *128*, 8384–8388

[1] X. Michalet, F. F. Pinaud, L. A. Bentolila, J. M. Tsay, S. Doose, J. J. Li, G. Sundaresan, A. M. Wu, S. S. Gambhir, S. Weiss, *Science* **2005**, *307*, 538–544.
[2] A. P. Alivisatos, W. W. Gu, C. Larabell, *Annu. Rev. Biomed. Eng.* **2005**, *7*, 55–76.
[3] F. Wei, G. Hu, Y. Wu, X. Wang, J. Yang, L. Liu, P. Zhou, Q. Hu, *Sens. Actuators B* **2016**, *229*, 38–46.
[4] E. Petryayeva, W. R. Algar, I. L. Medintz, *Appl. Spectrosc.* **2013**, *67*, 215–252.
[5] X. Gao, Y. Cui, R. M. Levenson, L. W. K. Chung, S. Nie, *Nat. Biotechnol.* **2004**, *22*, 969–976.
[6] T. Pons, E. Pic, N. Lequeux, E. Cassette, L. Bezdetnaya, F. Guillemin, F. Marchal, B. Dubertret, *ACS Nano* **2010**, *4*, 2531–2538.
[7] K. T. Yong, H. Ding, I. Roy, W. C. Law, E. J. Bergey, A. Maitra, P. N. Prasad, *ACS Nano* **2009**, *3*, 502–510.
[8] P. D. McNaughter, J. C. Bear, D. C. Steytler, A. G. Mayes, T. Nann, *Angew. Chem. Int. Ed.* **2011**, *50*, 10384–10387; *Angew. Chem.* **2011**, *123*, 10568–10571.
[9] H. Chibli, L. Carlini, S. Park, N. M. Dimitrijevic, J. L. Nadeau, *Nanoscale* **2011**, *3*, 2552–2559.
[10] S. Beyazit, S. Ambrosini, N. Marchyk, E. Palo, V. Kale, T. Soukka, B. Tse Sum Bui, K. Haupt, *Angew. Chem. Int. Ed.* **2014**, *53*, 8919–8923; *Angew. Chem.* **2014**, *126*, 9065–9069.
[11] M. Panagiotopoulou, S. Beyazit, S. Nestora, K. Haupt, B. Tse Sum Bui, *Polymer* **2015**, *66*, 43–51.
[12] V. C. Hascall, A. K. Majors, C. A. de la Motte, S. P. Evanko, A. Wang, J. A. Drazba, S. A. Strong, T. N. Wight, *Biochim. Biophys. Acta Gen. Subj.* **2004**, *1673*, 3–12.

[13] N. M. Varki, A. Varki, *Lab. Invest.* **2007**, *87*, 851 – 857.
[14] S. Seton-Rogers, *Nat. Rev. Cancer* **2012**, *12*, 228.
[15] C. Büll, M. A. Stoel, M. H. den Brok, G. J. Adema, *Cancer Res.* **2014**, *74*, 3199 – 3204.
[16] a) A. Kawamura, I. Kijima-Suda, M. Sugimoto, M. Itoh, K. Takada, K. Tomita, T. Ogawa, Y. Nagai, *Biochim. Biophys. Acta* **1990**, *1033*, 201 – 206; b) X. Xu, A. K. Jha, D. A. Harrington, M. C. Farach-Carson, X. Jia, *Soft Matter* **2012**, *8*, 3280 – 3294.
[17] a) M. J. Whitcombe, N. Kirsch, I. A. Nicholls, *J. Mol. Recognit.* **2014**, *27*, 297 – 401; b) L. Ye, *Adv. Biochem. Eng./Biotechnol.* **2015**, *150*, 1 – 24.
[18] L. Chen, X. Wang, W. Lu, X. Wu, J. Li, *Chem. Soc. Rev.* **2016**, *45*, 2137 – 2211.
[19] a) B. Tse Sum Bui, K. Haupt, *J. Mol. Recognit.* **2011**, *24*, 1123 – 1129; b) C. Baggiani, L. Anfossi, C. Giovannoli, *Mol. Imprinting* **2013**, *1*, 41 – 54.
[20] a) X. A. Ton, B. Tse Sum Bui, M. Resmini, P. Bonomi, I. Dika, O. Soppera, K. Haupt, *Angew. Chem. Int. Ed.* **2013**, *52*, 8317 – 8321; *Angew. Chem.* **2013**, *125*, 8475 – 8479; b) G. Ertürk, H. Özen, M. A. Tümer, B. Mattiasson, A. Denizli, *Sens. Actuators B* **2016**, *224*, 823 – 832; c) P. S. Sharma, Z. Iskierko, A. Pietrzyk-Le, F. D'Souza, W. Kutner, *Electrochem. Commun.* **2015**, *50*, 81 – 87.
[21] V. Pichon, F. Chapuis-Hugon, *Anal. Chim. Acta* **2008**, *622*, 48 – 61.
[22] a) B. Li, J. Xu, A. J. Hall, K. Haupt, B. Tse Sum Bui, *J. Mol. Recognit.* **2014**, *27*, 559 – 565; b) E. V. Piletska, B. H. Abd, A. S. Krakowiak, A. Parmar, D. L. Pink, K. S. Wall, L. Wharton, E. Moczko, M. J. Whitcombe, K. Karim, S. A. Piletsky, *Analyst* **2015**, *140*, 3113 – 3120.
[23] S. Kunath, M. Panagiotopoulou, J. Maximilien, N. Marchyk, J. Sänger, K. Haupt, *Adv. Healthcare Mater.* **2015**, *4*, 1322 – 1326.
[24] S. Shinde, Z. El-Schich, A. Malakpour, W. Wan, N. Dizeyi, R. Mohammadi, K. Rurack, A. G. Wingren, B. Sellergren, *J. Am. Chem. Soc.* **2015**, *137*, 13908 – 13912.
[25] a) D. Yin, S. Wang, Y. He, J. Liu, M. Zhou, J. Ouyang, B. Liu, H. Y. Chen, Z. Liu, *Chem. Commun.* **2015**, *51*, 17696 – 17699; b) S. Wang, D. Yin, W. Wang, X. Shen, J. J. Zhu, H. Y. Chen, Z. Liu, *Sci. Rep.* **2016**, *6*, 22757 – 22767.
[26] S. Nestora, F. Merlier, S. Beyazit, E. Prost, L. Duma, B. Baril, A. Greaves, K. Haupt, B. Tse Sum Bui, *Angew. Chem. Int. Ed.* **2016**, *55*, 6252 – 6256; *Angew. Chem.* **2016**, *128*, 6360 – 6364.
[27] A. Kugimiya, T. Takeuchi, *Biosens. Bioelectron.* **2001**, *16*, 1059 – 1062.
[28] A. G. Mayes, L. I. Andersson, K. Mosbach, *Anal. Biochem.* **1994**, *222*, 483 – 488.
[29] S. Xu, J. Ziegler, T. Nann, *J. Mater. Chem.* **2008**, *18*, 2653 – 2656.
[30] C. A. de la Motte, J. A. Drazba, *J. Histochem. Cytochem.* **2011**, *59*, 252 – 257.
[31] S. P. Evanko, W. T. Parks, T. N. Wight, *J. Histochem. Cytochem.* **2004**, *52*, 1525 – 1535.
[32] L. M. Steirer, G. R. Moe, *PLoS One* **2011**, *6*, e27249.

Received: January 31, 2016
Revised: March 17, 2016
Published online: May 30, 2016

